Research Article | Vol. 31, No. 21 / 9 Oct 2023 / Optics Express 34348
Optics EXPRESS

High-harmonic generation in liquids with few-cycle pulses: effect of laser-pulse duration on the cut-off energy

ANGANA MONDAL,[1] BENEDIKT WASER,[1] TADAS BALCIUNAS,[1] OFER NEUFELD,[2,3] ZHONG YIN,[1,4] NICOLAS TANCOGNE-DEJEAN,[2,3] ANGEL RUBIO,[2,3,5] AND HANS JAKOB WÖRNER[1,6]

[1]*Laboratory of Physical Chemistry, ETH Zürich, 8093 Zürich, Switzerland*
[2]*Max Planck Institute for the Structure and Dynamics of Matter, Luruper Chaussee 149, 22761 Hamburg, Germany*
[3]*Center for Free-Electron Laser Science CFEL, DESY, Notkestrße 85, 22607 Hamburg, Germany*
[4]*International Center for Synchrotron Radiation Innovation Smart, Tohoku University, 2-1-1 Katahira, 980-8577 Sendai, Japan*
[5]*Center for Computational Quantum Physics (CCQ), The Flatiron Institute, 162 Fifth Avenue, New York, NY 10010, USA*
[6]*hwoerner@ethz.ch*

Abstract: High-harmonic generation (HHG) in liquids is opening new opportunities for attosecond light sources and attosecond time-resolved studies of dynamics in the liquid phase. In gas-phase HHG, few-cycle pulses are routinely used to create isolated attosecond pulses and to extend the cut-off energy. Here, we study the properties of HHG in liquids, including heavy water, ethanol and isopropanol, by continuously tuning the pulse duration of a mid-infrared driver from the multi- to the two-cycle regime. Similar to the gas phase, we observe the transition from discrete odd-order harmonics to continuous extreme-ultraviolet emission. However, the cut-off energy is shown to be entirely independent of the pulse duration. These observations are confirmed by *ab-initio* simulations of HHG in large liquid clusters. Our results support the notion that the cut-off energy is a fundamental property of the liquid, independent of the driving-pulse properties. Our work implies that few-cycle mid-infrared laser pulses are suitable drivers for generating isolated attosecond pulses from liquids and confirm the capability of high-harmonic spectroscopy to determine the mean-free paths of slow electrons in liquids.

1. Introduction

Over the last two decades, high-harmonic generation (HHG) has established itself as a unique approach for producing attosecond pulses [1,2] and studying dynamics on electronic time scales [3,4]. HHG has also been successfully used as a probe for understanding strong-field dynamics in gases and solids with inherent attosecond time resolution. This has led to molecular-orbital tomography [5–7], time-dependent chirality [8–10], inter-band and intra-band electron dynamics [11–15] and probing of charge migration [16–18], to name a few. The basis of such applications of HHG to high-harmonic spectroscopy (HHS) is a clear understanding of the HHG mechanism. Such understanding has been achieved in gas-phase HHG through systematic studies of fundamental observables, e.g. how the cut-off energy scales as a function of laser parameters, such as intensity, wavelength, pulse duration [19–23]. However, most (bio)chemically-relevant reactions occur in the liquid phase, which motivates the exploration of HHG and HHS in liquids. Previous works on HHS have demonstrated bulk liquids to be a bright source of extreme-ultraviolet radiation [24–26]. To apply HHS to liquids, it is not only important to understand the HHG mechanism in liquids but also to systematically investigate how the harmonic spectrum depends

#496686 https://doi.org/10.1364/OE.496686
Journal © 2023 Received 7 Jun 2023; revised 31 Aug 2023; accepted 6 Sep 2023; published 29 Sep 2023

Optics EXPRESS

on various experimental parameters. Specifically, it is desirable to experimentally distinguish the properties of liquid-phase HHG that depend on the laser parameters from those that only depend on the inherent properties of the studied liquid.

In gas-phase HHG, the cut-off energy (E_c) depends on laser properties, i.e. intensity, wavelength and pulse duration [23,27–30]. The laser intensity (I) and wavelength (λ) govern the excursion of the electron trajectory in real space, resulting in the relation $E_c \propto I\lambda^2$. In thin media, such as gas jets, where propagation and phase-matching effects are negligible, this relation holds as long as ionization depletion is negligible. Because few-cycle pulses ionize a smaller fraction of the target, compared to multi-cycle pulses of the same peak intensity, few-cycle pulses achieve higher E_c [23,31]. Recent work on HHG from few-micron-thin liquid jets, including detailed phase-matching and absorption calculations [24], has demonstrated that the HHG signal builds up over the last few 100 nm of the liquid medium, comparable to the VUV/XUV absorption length of 10-100 nm [24]. As a result, similar to thin gas jets, the HHG in liquid flat-jets is unaffected by phase-matching conditions and is mainly governed by microscopic response of the high density liquid. Further experiments in liquid flat jets have confirmed these theoretical predictions and demonstrated that the cut-off energy E_c of the liquid harmonic spectra as defined by Lewenstein et al. [32], i.e. the end of the plateau region, is indeed independent of the driving wavelength and intensity [33]. Detailed *ab-initio* calculations and an intuitive semi-classical model show that the constant harmonic cut-off energy is a consequence of electron trajectory being limited by the electron mean-free path (MFP) [33], which is an inherent property of the liquid. In brief, HHG in liquids can be semi-classically described by a scattering-limited three-step-model. Similar to the gas phase HHG the incident laser pulse creates electrons that undergo large-amplitude laser-driven excursions within the medium before recombining with the valence holes, resulting in the emission of high harmonics. However, unlike gas-phase HHG, where the electron trajectory and therefore the cut-off energy strongly depends on driving wavelength and intensity, in liquids the maximum electron path length is limited by a characteristic electron MFP of the medium, which in turn depends on the inter-molecular distances (and potentially also other chemical and physical properties of the liquid such as its bonding character). Electrons following trajectories shorter than the MFP are able to return to the parent ion and recombine whereas electrons with longer trajectories are scattered, which suppresses recombination. This results in a wavelength-independent cut-off energy for the liquids that can be approximated by $3.73e(E_{peak}l_{max})/4$, where e is the elementary charge, E_{peak} is the peak electric field of the laser and l_{max} is the maximum excursion of the electron before being scattered. This semi-classical model captures the majority of the results observed both in experiments and through detailed *ab-initio* TDDFT calculations, providing an intuitive model and qualitative understanding of the HHG process in liquids. This is also in agreement with previous theoretical work, where liquids modelled as disordered linear chains of atoms in 1D and 2D have been used to simulate HHG in liquids [34–36]. The ab-initio calculations presented here and in [33], capture the actual three-dimensional structure of bulk liquids including all electrons and nuclei, and the chemical nature of the system. Further, the maximum harmonic energy ($E_{\max}$) in the multi-cycle regime has been shown to be linearly dependent on the electric-field amplitude [24,33]. As a direct consequence of the dominance of microscopic effects in liquid-flat-jet HHG, the cut-off energy is predicted to have a weak dependence on the laser pulse duration. However, in contrast to all of these considerations and detailed investigations, recent work in liquid-phase isopropanol in the few-cycle regime [37], claims the maximum energy of harmonic spectra (designated as cut-off energy) to be strongly-linearly dependent on the laser intensity with cut-off energies as high as ~50 eV. Both properties are reminiscent of gas-phase HHG on one hand [28], and contrast markedly with previous work on liquid-phase HHG [24–26,33,34] on the other. These observations have led the authors of Ref. [37] to the conclusion that electron-scattering cross sections in liquid isopropanol must be much smaller than those of isolated isopropanol molecules

Optics EXPRESS

in the gas phase. However, in an earlier work utilizing few-cycle pulses of a 800 nm driver, an extension of the cut-off energy was not observed [25]. These interesting controversies additionally motivate the present work.

Here, we demonstrate the influence of pulse duration of liquid-phase HHG by presenting back-to-back measurements of liquid- and gas-phase high harmonics in the two-cycle regime of 1.8 μm laser wavelength. Our results clearly show that the cut-off energy (E_c) remains pulse-width independent with a very weak to nonexistent dependence on intensity in the case of the liquid-phase high-harmonic spectrum throughout the transition from the multi-cycle ($\sim$ 50 fs) to the two-cycle regime ($\sim$ 11.5 fs) regime. In comparison, the gas-phase harmonics show the expected linear dependence on the laser intensity for both E_c and E_{max}. We further demonstrate the pulse-width independence of E_c to be a general property of harmonic spectra generated from ethanol, isopropanol and heavy water (D_2O). Our work provides a novel, and completely independent confirmation of the fact that E_c in liquid-phase high-harmonic spectra is a fundamental property of the liquids, limited by the electron mean-free paths, and is weakly influenced by laser parameters, such as wavelength, pulse duration or intensity. These observations are confirmed by *ab-initio* calculations of HHG in liquids [38]. Consistent with the scattering model introduced in Ref. [33], the experimental and numerical results demonstrate that even in the few-cycle regime, the experimental results can be fully explained in terms of electron scattering as the limiting factor determining E_c for harmonics generated in the liquid phase. Considering previous results in combination with our current findings allows us to decouple the effect of the driving laser parameters like intensity, wavelength and pulse duration completely and use high harmonic spectroscopy to investigate microscopic properties of the bulk liquids themselves. In addition, as inferred from the continuity of the harmonic spectra, the experimental results suggests liquid-phase HHG as a source of attosecond extreme-ultraviolet pulses at much lower threshold intensities in comparison to the gas phase.

2. Experimental setup

A commercial 0.8 μm, 1-kHz Ti-Sapphire laser coupled with an optical parametric amplifier HE-TOPAS is used to generate 800 μJ laser pulses centered at 1.8 μm with a duration of 43 fs (blue trace in Fig. 1 (D)). The 1.8 μm pulses are generated using the idler beam from the parametric amplifier in a configuration where the pulses are passively carrier-envelope phase (CEP) stable [39]. However, the CEP has not been corrected for long-term drifts. Nevertheless, the CEP is expected to be stable over the period of acquisition of a single HHG spectrum (600 ms). These pulses are then coupled into a hollow-core fiber (HCF) of 703 μm inner diameter with a 1.5 m focal length lens. The HCF is filled with 2.4 bar of Ar to generate a broadened optical spectrum as shown by the orange trace in Fig. 1(B). A pulse width of $\sim$ 25 fs is obtained from the output of the HCF (orange trace in Fig. 1 (D)). Further compression is provided by the 2 mm fused silica window of the experimental chamber resulting in the two-cycle pulse (yellow line in Fig. 1 (D)). These pulses are then focused on a liquid flat-jet of $\sim$ 1 μm thickness with a concave mirror of 40 cm focal length. The generated harmonics are diffracted by a XUV grating onto a multi-channel plate (MCP) backed with a phosphor screen that is captured by an optical CCD camera for detection.

The flat-jet, formed by the colliding jet geometry [24] is mounted on an XYZ manipulator for finer adjustment with respect to the laser beam. The gas target is delivered using a heatable bubbler mounted on the same XYZ stage at a distance of 2.5 cm from the flat-jet. We can therefore measure the gas-phase harmonics by simple translation along the lateral direction. The MCP is maintained at a voltage of -1.6 kV and the phosphor at 3.3 kV for detection of the liquid-phase harmonic spectra with an acquisition time of 200 ms. Each data set is then averaged over 30 such spectra. As the signal yield from the gas-phase harmonics is lower, the MCP voltage is increased to -1.7 kV with an acquisition time of 600 ms and 30 spectra are

Optics EXPRESS

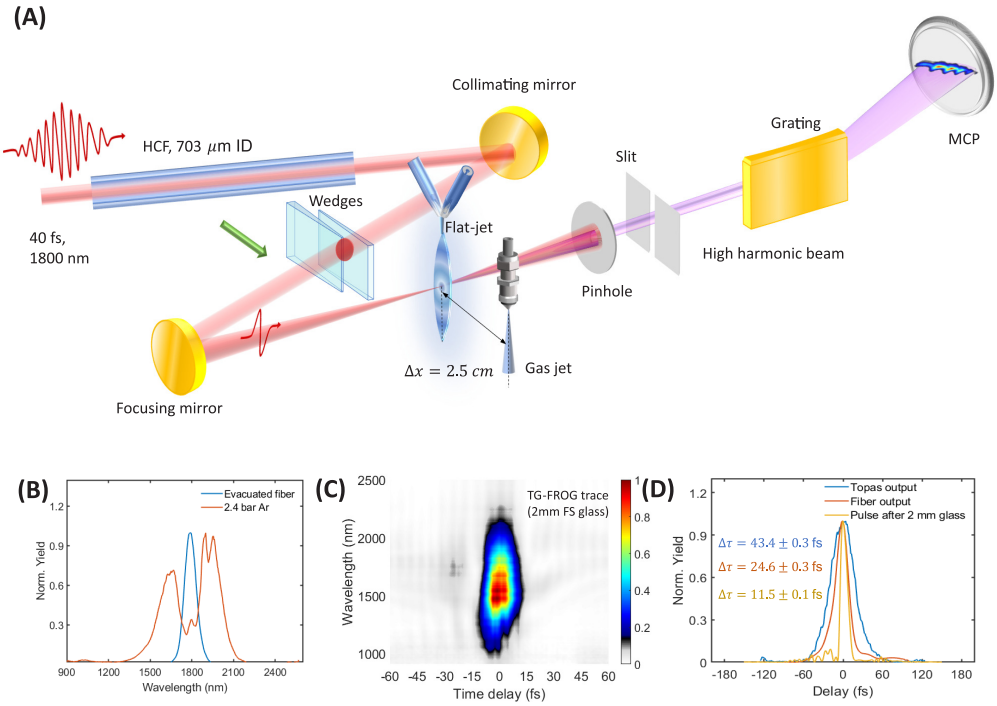

Fig. 1. (A) Schematic of the experimental setup. Laser pulses with a central wavelength of 1800 nm, pulse energy of 800 μJ and pulse width of ~43 fs are focused into a HCF of 703 μm inner diameter filled with 2.4 bar Ar. The exiting broadened pulse passes through a 2-mm fused-silica window before being focused on the flat-jet target for generating high harmonics. The harmonics pass through a slit into the XUV spectrometer that diffracts the different orders onto an MCP backed with a phosphor screen. The gas-phase sample is delivered into the laser beam through a heatable bubbler coupled to a nozzle. This setup is mounted on the same 3D manipulator as the liquid jet, such that back-to-back measurements of liquid- and gas-phase samples can be realized by a lateral translation of 2.5 cm. (B) A comparison of the unbroadened IR spectrum obtained from an evacuated fiber (blue line) and the broadened IR spectrum in presence of 2.4 bar Ar (orange line). (C) The transient-grating FROG trace of the compressed laser pulses. (D) Comparison of FWHM pulse-profiles measured using FROG for the initial TOPAS output (blue line), at the output of the fiber (orange line) and after the 2 mm FS window (yellow line). FWHM widths obtained from Gaussian fits are indicated in the plot.

averaged in the case of the gas-phase data. The pulse width variation was performed using a pair of fused-silica wedges, where one wedge is kept fixed while the other was translated with an automated stage. This varied the amount of additional glass in the beam path from ~0.51 mm to ~1.72 mm. Beyond this, an additional 2 mm fused-silica window was added in the beam path to vary the glass thickness from 2.5 mm to 3.72 mm over the same range of wedge displacements.

3. Results and discussion

Figure 1(A) shows a schematic of the experimental setup used to generate the 1.8 μm few-cycle laser pulse. Figure 1 (B) shows the unbroadened IR spectrum for the case of an evacuated fiber (blue line), corresponding to a multi-cycle pulse with a measured pulse duration of ~ 43 fs, i.e. a Fourier-limited pulse. The harmonic spectrum generated from such a multi-cycle pulse is

Optics EXPRESS

expected to consist of discrete harmonics as a consequence of the time-periodicity of the HHG process. A spectral broadening of the 1.8 μm laser pulse, shown as orange line in Fig. 1 (B), is obtained by filling the HCF with 2.4 bar of Ar. The broadened pulse is then propagated through 2 mm of fused silica (FS) (experimental chamber window) before hitting the liquid jet. This results in a compressed pulse of ~11.5 fs full-width at half maximum (FWHM) as shown by the yellow trace in Fig. 1(D), using a Transient-Grating Frequency-Resolved Optical Gating (TG-FROG) [40] measurement (Fig. 1(C)). As one approaches the single-cycle regime, the discrete harmonic spectrum is expected to evolve into a continuous one [23].

3.1. Observation of high-harmonic generation from bulk liquids using two cycle pulses

Figure 2(A) shows a comparison of the harmonic spectrum obtained from the multi-cycle pulse (blue line) and from a two-cycle pulse (orange line), where a clear transformation of the discrete harmonic spectrum to a continuous one is observed. For the reported liquid-phase spectra the laser intensity is kept below the onset of plasma generation, where plasma lines are no longer visible in the recorded spectra (Supplement 1, Fig. S1). To measure a systematic intensity dependence of the harmonic spectra in the liquid phase it is essential to eliminate possible gas-phase contributions from the liquid harmonic spectrum. Therefore, it is essential to do a back-to-back measurement of both gas and liquid phases separately to exclude gas-phase contributions to the liquid-phase harmonics. Generally, a reference gas spectrum can be obtained by simply translating the flat-jet laterally [24,25,33]. As evaporation from the flat-jet creates a gas-phase background, this method is sufficient for acquiring gas-phase spectra up to 1500 nm wavelength [24]. However, we observed that at 1800 nm (both for multicycle and single cycle regime) no detectable gas-phase harmonic signal were present when the laser was focused 0.5 mm (about the lateral size of the flat jet) away from the center of the jet where the gas-phase signal was measured for shorter wavelengths [33]. This can directly be inferred from the acquisition times of the signal. For harmonic spectra obtained with an 800-nm driver, a gas-phase harmonic spectrum (acquired by a lateral 0.5 mm shift from the jet center) requires an acquisition time of 200 ms, whereas similar signal intensity for the liquid-phase harmonic spectra only takes 20 ms [33]. For the current 1800-nm measurements a collection time of 200 ms was required to obtain the liquid spectrum with decent signal-to-noise ratio. In agreement with previous measurements, this would require an acquisition time of 2000 ms for the gas-phase spectrum, which is beyond the maximum acquisition time of the system.

However, this observation reported independently for few-cycle measurements done on liquid isopropanol [37], is not sufficient to rule out gas-phase contribution in the liquid-phase harmonic spectra. At 1800 nm and under the chosen focusing conditions, the Rayleigh range amounts to $\sim$ 1 cm. Therefore, at sufficiently high laser intensities, the laser beam passing through the jet has enough intensity to generate harmonics from the gas layer adjacent to the back surface of the liquid jet. The gas density indeed monotonically decreases with the distance from the liquid-gas interface. In addition, the driving laser itself causes heating of the liquid, which increases evaporation resulting in an increased gas density for the next arriving laser pulse. This effect is absent when we laterally shift the flat-jet out of the interaction region. To overcome these challenges and successfully realize a back-to-back measurement of the gas- and liquid-phase harmonics a heatable bubbler has been designed and mounted on the flat-jet XYZ manipultor stage at a distance of 2.5 cm from the flat-jet, which is five times the spatial lateral extension of the flat jet. This ensures that identical incident laser parameters for harmonic generation from gas and liquid phases are achieved just by a lateral translation. Since the high-harmonic signal from gases is dependent on the position of the target with respect to the laser focus [41,42], the comparative study was performed at a position where the maximum signal intensity of gas-phase harmonics was observed.

Optics EXPRESS

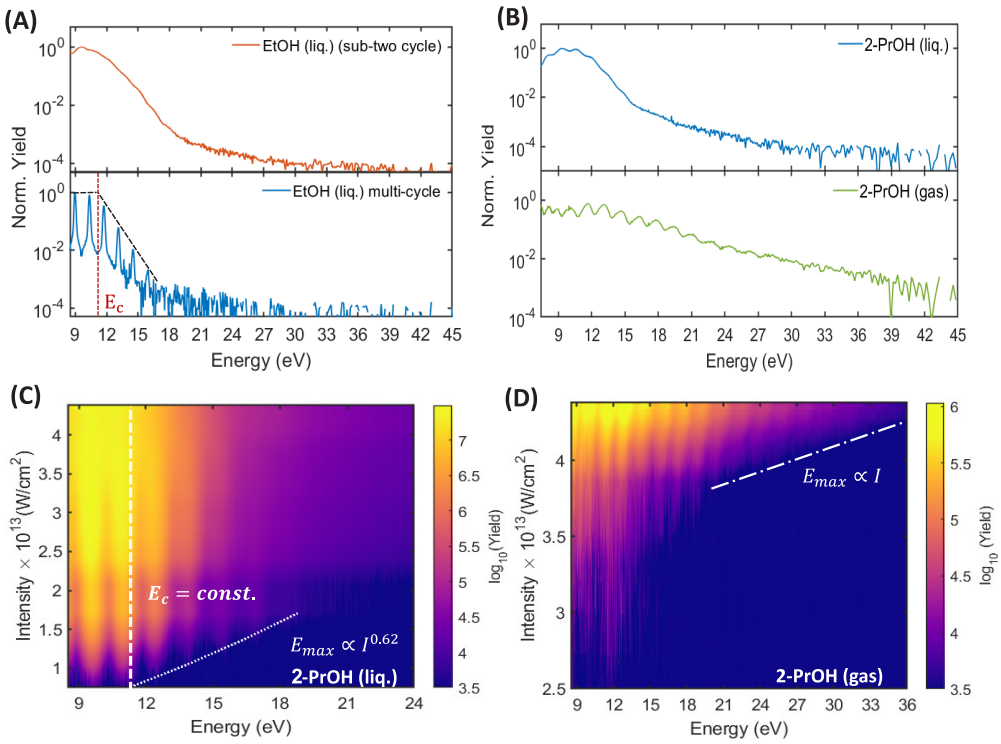

Fig. 2. (A) A comparison of the high-harmonic spectrum from the uncompressed laser pulse (IR beam passing through evacuated fiber) (blue line) and the compressed two cycle laser pulse (IR beam passing through the fiber filled with 2.4 bar Ar, orange line). The XUV spectrometer used can measure harmonics down to 5 eV. In the current experiments the MCP has been shifted to better access the higher-energy harmonics of the gas phase, setting a lower energy limit of 8.2 eV. An ethanol HHG spectrum extending down to 5 eV is shown in the Fig. S5, Supplement 1. (B) A comparison of the harmonic spectrum generated from liquid-phase isopropanol (blue line) and gas-phase isopropanol (green line) using two-cycle 1.8μm, ~ 12 fs laser pulses. (C) Harmonic spectra from liquid-phase isopropanol for a range of intensities driven by two-cycle pulses. (D) Harmonic spectra from gas-phase isopropanol for a range of intensities driven by two-cycle pulses, under identical experimental conditions of the liquid measurements.

Isopropanol was chosen as the target for the liquid and gas-phase comparative study due to its higher vapor pressure as compared to water, which makes it easier to form a denser gas jet. Figure 2(B) shows a comparison of the normalized harmonic spectrum generated from isopropanol in gas- (green line) and liquid-phase (blue line) with a two-cycle 1800 nm laser pulse with a peak intensity of 4.4×10^{13} space W/cm^2. As expected, we observe that the liquid E_c of ~ 11.3 eV (determined using the technique elaborated in section 3.2, consistent with the Lewenstein definition [32]). Furthermore, it is observed that the maximum photon energy for the gas-phase spectrum extends up to 35 eV, whereby the detection limit is determined by the background signal. A closer inspection of the liquid-phase isopropanol spectrum in Fig. 2(B) (top panel) beyond the range of 17 eV shows a similar slope of harmonic yield vs. photon energy as compared to the gas-phase-only spectrum in Fig. 2(B) (bottom panel). This is indicative of competing gas-phase signal in the liquid jet spectra for energies beyond 17 eV. A detailed comparison of the measured liquid- and gas-phase-only isopropanol spectra at few selected

Optics EXPRESS

intensities is presented in Fig. S2 (C), Supplement 1 where the blue line shows the harmonic signal from the liquid jet and the orange line denotes the harmonic signal from gas only and the yellow line shows liquid-only the spectrum (liquid jet - gas only). We have to keep in mind here that the gas-phase high-harmonic signal generated by the heated bubbler target is significantly higher and therefore detectable as compared to that generated by spontaneous and laser-induced evaporation of the liquid jet, mostly because of the lower gas density in the latter cases. Even then, as can be seen, due to the difference in magnitude of the emitted harmonic signal, the cut-off energy of ~11.3 eV (end of plateau, following the Lewenstein definition) remains unaffected by the addition of the gas-phase signals. However, the harmonics beyond ~ 17 eV in the gas phase and liquid phase signals are comparable. Therefore, while the end of the plateau region can be strictly attributed to the harmonics from liquids alone, this does not hold true for the maximum energy of the harmonic spectrum. Further, as the cut-off energies for gases scale linearly with intensity, convolution of gas-phase harmonic spectra in the liquid jet measurements can introduce a pseudo-linear dependence of the maximum harmonic energy of the high-harmonic spectra on the laser intensity.

To observe the effect of pulse duration on the HHG cut-off energy of liquids, a systematic variation of the pulse duration was performed using a pair of fused-silica wedges. Since the pulse energy and focal spot size are kept constant during the pulse-duration measurement, the pulse duration is also coupled to the intensity of the laser pulse incident on the liquid jet. In order to decouple the intensity from the pulse-duration effects, we first performed an intensity scan at a constant pulse duration of ~ 12 fs. The intensity variation at a fixed pulse duration is varied with the help of an automated iris. At each iris position the focal spot size is imaged and the transmitted beam power is measured. As the harmonic spectra are acquired at a distance of 11 mm from the focus position, the $1/e^2$ radius is calculated using

$$w(z) = w_0\sqrt{1 + (\frac{z}{z_R})^2} \tag{1}$$

where w_0 is the $1/e^2$ radius of the beam at focus, z is the distance from the focus, z_R is the Rayleigh length for specific w_0 and $w(z)$ is the $1/e^2$ radius of the beam at distance z from the focus. For a gaussian beam 99% of the beam power is contained in an area of radius $w'(z) = 1.52w(z)$. The respective intensity of each aperture diameter is calculated as

$$I = \frac{2P}{\pi w'(z)^2 t} \tag{2}$$

where P is the total power transmitted through the iris, t is the FWHM pulse duration of ~12 fs. Figure 2(C) shows the harmonic spectra from liquid isopropanol over a range of laser intensities. The calculated intensities are expected to be accurate within a relative error of 20%. We find that in the liquid phase harmonic generation already occurs for intensities as low as 1×10^{13} W/cm^2 and that E_c is constant at ~11.3 eV, independent of the incident intensity. Another interesting observation is that with increasing intensity the liquid harmonic spectra evolve from discrete to continuous.

In comparison to the liquids, Fig. 2(D) shows the normalized harmonic spectrum of gas-phase isopropanol for similar intensities. It is observed that gas-phase harmonics appear only above a threshold intensity of ~3.8×10^{13} W/cm^2 and, as expected, E_{max} shows a linear dependence on the incident laser intensity .

3.2. Pulse-width dependence of cut-off energy for different liquids

The intensity-dependent measurements in the few-cycle regime (Fig. 2(C)) establishes that for liquid-phase harmonic generation the cut-off energy is very weakly (if at all) dependent on the

Optics EXPRESS

laser intensity, which is consistent with the observations made in the multi-cycle regime [33]. As a result, any observed effect in the cut-off energy of the liquid harmonic spectra as a function of the pulse duration can now be directly attributed to the pulse-width effect. A systematic variation of the pulse duration was performed using a pair of fused-silica wedges, where one wedge was fixed and the other one was translated using an automated stage.

The pulse duration at each wedge thickness is measured using TG-FROG, as shown in Fig. 3(A). The black dashed line indicates the quadratic fitting of the pulse-duration as a function of glass thickness that is used for calibrating the pulse durations for Fig. 3(B). Figure 3(B) shows the harmonic spectrum obtained from liquid isopropanol for different pulse durations. The normalized harmonic spectra have been vertically displaced for clarity. These data sets were taken at a fluence of 0.56 J/cm^2 corresponding to a maximum intensity of 4.27×10^{13} W/cm^2, for a 13-fs pulse duration. A clear transition from a slightly modulated continuous spectrum to a sharply peaked odd-only harmonic spectrum at higher pulse durations is observed. We also observed a red shift in the high-harmonic peaks with decreasing pulse duration. This is the consequence of a higher-order phase effect introduced by the fused silica wedges. A detailed discussion and simulations of the observed peak shift with the variation of fused silica thickness is presented in the Supplement 1 (Fig. S3).

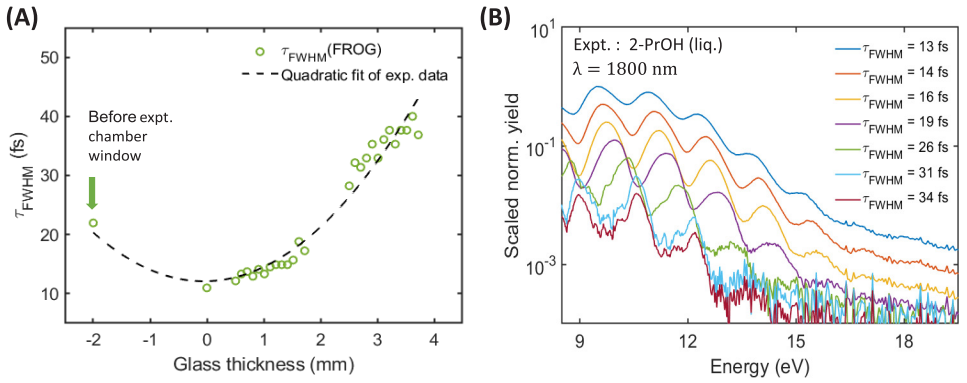

Fig. 3. (A) Quadratic fit of experimentally measured FROG data to calibrate pulse width (FWHM) as a function of glass thickness. The data point at -2 mm glass thickness corresponds to the FROG measurement at the output of the HCF before transmission through the 2 mm FS experimental chamber window. (B) Harmonic spectra from liquid-phase 2-PrOH for different glass thicknesses. The normalized harmonic spectra at different pulsewidths have been vertically displaced for better visualization.The data sets were taken at a fluence of 0.56 J/cm^2 corresponding to a maximum intensity of 4.27×10^{13} W/cm^2, for 13 fs pulse duration.

Another interesting phenomenon is observed at intermediate pulse durations, e.g. in the green, blue and maroon curves of Fig. 3(B), corresponding to pulse durations of 26 fs, 31 fs and 34 fs, respectively. In these cases, the harmonic peaks display a substructure that is best visible around 12 eV. This substructure is attributed to the interference of the direct, forward-propagating emission from the bulk liquid with a replica that has been internally reflected twice before exiting the thin liquid sheet. This assignment is supported by the photon-energy intervals of the observed structure and our previous work on the subject [25]. Importantly, we find here that these substructures disappear for shorter pulse durations, resulting in the generation of truly continuous XUV spectra. This, in turn, indicates that isolated attosecond pulses with a good temporal contrast could be generated from liquids.

Finally, we also investigated whether the liquid-phase E_c changes as a function of pulse duration for different liquids. For this purpose we compare the nearly continuous harmonic

Optics EXPRESS

spectrum obtained for a glass thickness of 0.51 mm with the harmonic spectrum obtained for the maximum glass thickness of 3.72 mm. Figure 4(A) shows the temporal profiles of the laser pulses measured using FROG for these two glass thicknesses at a fluence of ~ 0.51 J/cm^2. Figure 4(B), Fig. 4(C) and Fig. 4(D) show that E_c is independent of pulse duration for liquid-phase ethanol, isopropanol and heavy water with their cut-off energies amounting to 11.1 eV, 11.3 eV and 12.9 eV, respectively, within an accuracy of one harmonic order. To determine the cut-off energy (end of the plateau region) accurately in the discrete multi-cycle liquid harmonic spectrum and reduce human errors, we uses the approach elaborated in Figure S2 of [33].

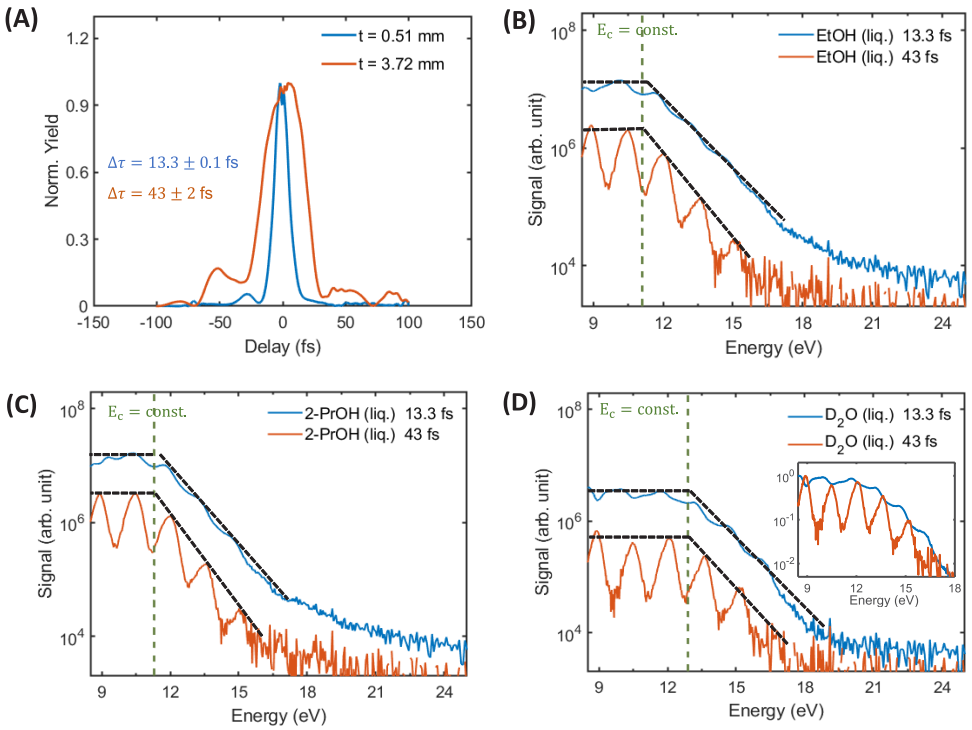

Fig. 4. (A) Measured temporal profiles of the two-cycle pulse after it propagates through 0.51 mm FS (blue line) and 3.72 mm (orange line). FWHM widths obtained from Gaussian fits are indicated in the plot. (B-D) Harmonic spectra from liquid-phase ethanol (B), isopropanol (C) and D_2O (D) for different glass thicknesses Inset in Fig. 4(D) shows the same spectra as Fig. 4(D) but normalized. The 13.3 fs spectrum is seen to envelope the 43 fs spectrum indicating negligible shift in cut-off energy. The black dased lines in all figures of Fig. 4 are guides for the eye while the green dashed lines indicate the cut-off energy determined for the multi-cycle spectrum using the fitting technique described in the manuscript.

In brief, we explain the methodology as follows. A typical harmonic spectrum (beyond the perturbative regime) for a multi-cycle laser pulse includes a plateau region with harmonic peaks of comparable signal strength, followed by a cut-off region where the harmonic yield falls off exponentially as a function of harmonic order. This is observed as a linear decline on a log-linear scale as shown in Fig. 4(B-D). We perform a linear fitting of the logarithm of the signal at each harmonic peak in the cut-off region as a function of the harmonic energy (represented by the black-slanted dashed lines in the orange curves of Fig. 4(B-D)). The black dashed lines parallel to the energy axes in the orange curves of Fig. 4(B-D) represent the average intensity value of the plateau harmonics. The intersection of these two lines (the average log(signal) of plateau

Optics EXPRESS

harmonics and the linear fit of the log(signal) for the cut-off harmonics), is denoted the cut-off energy and is depicted by the green dashed lines in Fig. 4(B-D). Since the spectrum is continuous in the few-cycle regime, we do not observe discrete peaks but rather a slight modulation on top of a continuous spectrum. Overlaying the normalized spectrum of the few-cycle driver with that of the multi-cycle driver (inset of Fig. 4(D)) we see that the continuous spectrum (blue line for 13.3 fs) envelopes the discrete spectrum (orange line for 43 fs) perfectly, indicating a negligible change in the cut-off energy.

3.3. Ab-initio calculations

As discussed in the introduction, the HHG intensity in liquid flatjets builds up over the last few 100 nm, as shown in the multi-cycle regime [24]. In the present work, we found that the cut-off energy is observed to be independent of the laser pulse duration, which we therefore attribute to a microscopic effect of HHG in the liquid phase. The observed cut-off clamping effect can moreover not be a result of the XUV absorption in the liquid bulk. We demonstrate this by comparing HHG spectra to the XUV absorption curve of water, shown in Fig. S4, Supplement 1 calculated from $\alpha(E) = 4\pi Ek(E)/hc$, where E is the photon energy, $k(E)$ is the imaginary part of the refractive index of liquid phase water as a function of the photon energy, taken from [43]. Comparing this curve to the HHG spectrum obtained from liquid D_2O (Fig. 4 (D)), we see that the cut-off energy of $\sim$ 14 eV cannot be explained in terms of the absorbance curve.

As a further confirmation of the microscopic origin of the cut-off clamping with laser pulse duration, we employ the recently developed methodology for calculating the HHG response of liquids through the use of finite-sized clusters [38]. We use 54-molecule water clusters for calculating the nonlinear optical response, which is further averaged over 14 orientations. Our simulations are based on the framework developed in Ref. [38]. The cluster approach attempts to passivate the surface contribution to the harmonic response by an additional absorbing layer placed outside of the cluster, and by freezing the surface state dynamics. The resulting HHG response approximately corresponds to that of the bulk liquid.

We model the laser-matter interaction in the length gauge with the following electric field:

$$E(t) = E_0 f(t) \cos(\omega t + \phi_{CEP}) \tag{3}$$

where E_0 is the field amplitude, ω is taken to correspond to an 1800 nm driving wavelength, $f(t)$ is an envelope function taken as a super-sine form [44], which roughly corresponds to a super-Gaussian but is numerically more convenient, and ϕ_{CEP} is the carrier-envelope phase (CEP). We modeled several different pulse durations corresponding to different HHG regimes, using a 1800 nm driving wavelength. For the long-pulse limit we used a FWHM of 24 fs and a peak pulse intensity of 2.625×10^{13} W/cm^2, and the CEP was set to zero. The shorter pulse durations employed a peak pulse intensity that was increased linearly with respect to the pulse duration, roughly corresponding to the experimental settings. The response was further averaged over three CEPs of values of 0, $\pi/4$, and $\pi/2$, to correspond to the experimental set-up which is not long-term CEP-stabilized. Figure 5(A) shows the numerically obtained spectra for several pulse durations, which correspond very well with the experimental results in Fig. 5(B). The residual harmonics observed in Fig. 5(A) and (B) are not integer harmonics and likely result from averaging over only 3 CEP values in the theory.

Indeed, the cut-off in the *ab-initio* calculations is independent of the pulse duration, and is very weakly dependent on the pulse peak power (increasing by only 1 eV when the peak intensity is increased by a factor of 4). Moreover, the calculations show that the harmonic peak contrast indeed decreases when employing shorter pulses, as observed experimentally. Further, decoupling the effects of pulsewidth and intensity, Fig. 5 (C) shows the harmonic spectrum from the *ab-initio* calculation for two different pulse durations at a fixed intensity of 6×10^{13} W/cm^2, which also shows a fixed cut-off energy for both the 6 fs and 10.5 fs spectra. As the cut-off

Optics EXPRESS

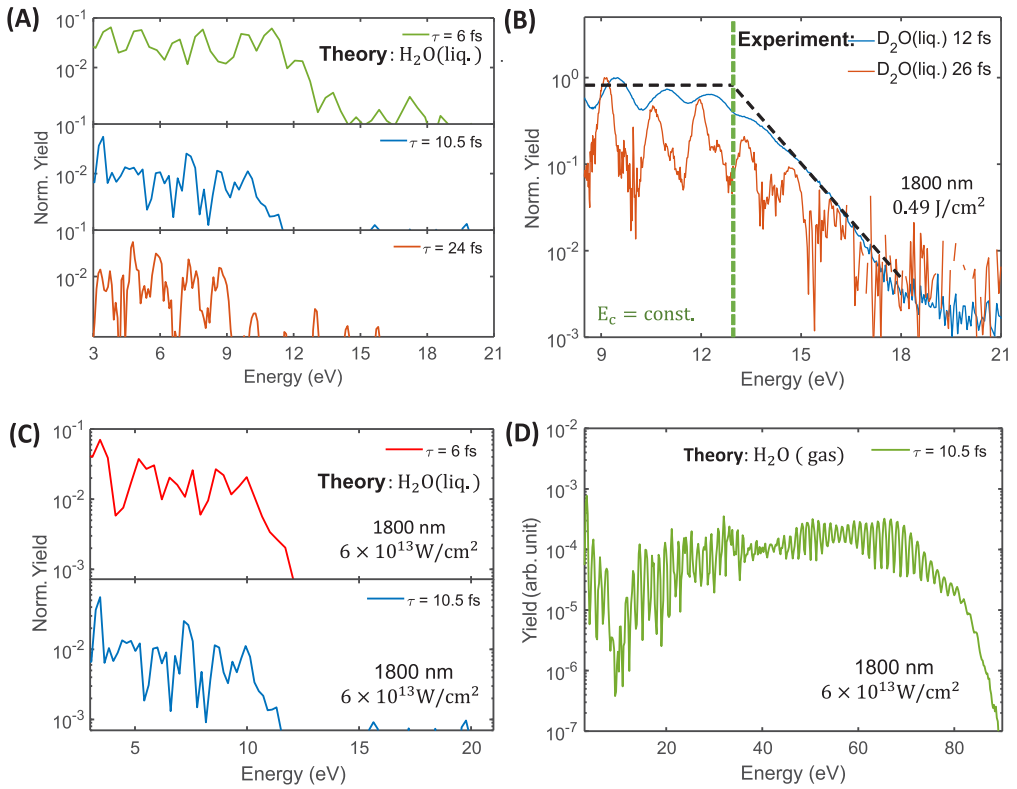

Fig. 5. (A) Harmonic spectra for different (6 fs, 10.5 fs and 24 fs) pulse durations for liquid phase H_2O obtained from *ab-initio* calculations. The calculations were performed at a fluence of 0.63 J/cm^2. (B) Experimental harmonic spectra of liquid D_2O at similar pulse duration as the *ab-initio* calculations at a fluence of 0.49 J/cm^2. The dashed lines are guides for the eye indicating the cut-off energy position. (C) Harmonic spectra for different (6 fs and 10.5 fs) pulse durations for liquid-phase H_2O obtained from *ab-initio* calculations at a fixed laser intensity of 6×10^{13} W/cm^2. (D) High harmonic spectrum for gas-phase H_2O from *ab-initio* calculations for 1800 nm wavelength, 10.5 fs pulse duration at an intensity of 6×10^{13} W/cm^2.

clamping effect is reproduced by the *ab-initio* TDDFT calculations, which do not include self absorption or propagation effects in the liquid, it provides additional verification that the above experimental findings are a signature of the microscopic mechanism in the liquid phase and not the result of macroscopic effects. Overall, these results agree well with our previously developed semi-classical trajectory model [33] that predicts a similar weak dependence on pulse peak power due to a suppression of longer electron trajectories through mean-free-path-limited scattering channels in the liquid. Such a strong suppression is not observed in the gas-phase calculations, which follow the expected simple three-step-model results as seen in the gas-phase simulations of Fig. 5 (D).

4. Discussion

We have previously argued that, in the multi-cycle regime, HHG from liquids is well explained by a scattering-limited trajectory model. Based on this trajectory picture, E_c is determined by the characteristic electron mean-free path (MFP) in a liquid, which is shown to be comparable to the electron MFP in liquid water, methanol, ethanol and isopropanol [33]. Determining MFPs

Optics EXPRESS

for few-eV electrons in the liquid phase is an unsolved challenge, both computationally and experimentally. As a result, reliable low-energy electron MFPs have so far only be obtained in liquid H_2O through a combination of experimental and theoretical methods [45,46]. For the alcohols, the liquid-phase MFP has been estimated by $1/(n\sigma)$, where σ is the gas-phase elastic scattering cross-section and n is the number density of scattering molecules in the liquid phase. The agreement of the MFP values derived from the scattering-limited trajectory model for the multi-cycle liquid-jet experiments [33] and the estimated MFP values proved that scattering played the decisive role for determining E_c for liquids. As a result, unlike in gases E_c is observed to be wavelength- and approximately intensity-independent in the multicycle regime. These observations are also consistent with a previous theoretical study of liquid-phase HHG, where liquids were modeled using a linear chain of disordered atoms and the cut-off energy was related to a coherent travel distance [34].

In this work we have demonstrated that the cut-off energies (end of the plateau) obtained for different liquids in the current experiments using two-cycle pulses are also in agreement with the multi-cycle measurements obtained with driving wavelengths of 800 nm, 1500 nm and 1800 nm on liquid flat-jets [33] and is demonstrated to be intensity-independent above a certain threshold intensity. Through a systematic variation of the pulse duration, we have observed that harmonic spectra from liquids evolve from continuous to discrete with increasing pulse duration. The observed behavior is consistent with the scattering model of HHG in liquids. Since E_c is solely dependent on the liquid MFP and independent of the intensity, the increase in pulse duration just causes the transition of the harmonic spectrum from continuous to discrete. These results further demonstrate that even in the two-cycle regime, scattering plays the dominant role in the HHG mechanism in liquids, and the simple conceptual model developed in Ref. [33] is valid. Furthermore, with a back-to-back measurement of gas-phase and liquid-phase isopropanol with two-cycle pulses, we showed that for liquids E_c remains intensity independent as opposed to the expected linear intensity dependence in the gas-phase spectra. We also showed that the onset of HHG in bulk liquid isopropanol occurs at much lower peak intensities (1×10^{13} W/cm^2) compared to the gas phase (3.8×10^{13} W/cm^2).

The present results thus show that two-cycle mid-infrared driving pulses generate fully continuous XUV spectra from bulk liquids. However, unlike in gas-phase HHG, the cut-off energy is not extended, but on par to that obtained with multi-cycle drivers. Combined with our previous results demonstrating the wavelength-independence of the cut-off energy E_c in the multi-cycle regime, the present results further confirm that scattering plays a dominant role in HHG in liquids making E_c a fundamental property of the liquid, independent of laser parameters such as wavelength, intensity and pulse duration. Owing to the continuous nature of the emitted XUV spectra which enable a more accurate determination of E_c, few-cycle HHG in liquids may become an accurate method for the first all-optical determination of the mean-free paths of slow electrons in liquids, which play an important role in the understanding of radiation damage in aqueous environments. Additionally, our results suggest that HHG in liquids may become an efficient source of isolated attosecond pulses for driving lasers with limited peak intensities, such as oscillators with megahertz repetition rates.

Funding. Eidgenössische Technische Hochschule Zürich; Schweizerischer Nationalfonds zur Förderung der Wissenschaftlichen Forschung (200021_204928).

Acknowledgments. The authors thank Andreas Schneider and Mario Seiler for their contributions to the construction and improvements of the experimental setup.

Disclosures. The authors declare no conflicts of interest.

Data availability. Data underlying the results presented in this paper are not publicly available at this time but may be obtained from the authors upon reasonable request.

Supplemental document. See Supplement 1 for supporting content.

Optics EXPRESS

References

1. M. Hentschel, R. Kienberger, C. Spielmann, G. A. Reider, N. Milosevic, T. Brabec, P. Corkum, U. Heinzmann, M. Drescher, and F. Krausz, "Attosecond metrology," Nature **414**(6863), 509–513 (2001).
2. P. M. Paul, E. S. Toma, P. Breger, G. Mullot, F. Augé, P. Balcou, H. G. Muller, and P. Agostini, "Observation of a train of attosecond pulses from high harmonic generation," Science **292**(5522), 1689–1692 (2001).
3. M. Drescher, M. Hentschel, R. Kienberger, M. Uiberacker, V. Yakolev, A. Scrinzi, T. Westerwalbesloh, U. Kleineberg, and F. Krausz, "Time-resolved atomic innershell spectroscopy," Nature **419**(6909), 803–807 (2002).
4. K. Klünder, J. M. Dahlström, M. Gisselbrecht, T. Fordell, M. Swoboda, D. Guénot, P. Johnsson, J. Caillat, J. Mauritsson, A. Maquet, Taïeb, and A. L'Huillier, "Probing single-photon ionization on the attosecond time scale," Phys. Rev. Lett. **106**(14), 143002 (2011).
5. J. Itatani, J. Levesque, D. Zeidler, H. Niikura, H. Pépin, J. C. Kieffer, P. B. Corkum, and D. M. Villeneuve, "Tomographic imaging of molecular orbitals," Nature **432**(7019), 867–871 (2004).
6. S. Haessler, J. Caillat, W. Boutu, C. Giovanetti-Teixeira, T. Ruchon, T. Auguste, Z. Diveki, P. Breger, A. Maquet, B. Carré, R. Taïeb, and P. Salières, "Attosecond imaging of molecular electronic wavepackets," Nat. Phys. **6**(3), 200–206 (2010).
7. P. Peng, C. Marceau, and D. M. Villeneuve, "Attosecond imaging of molecules using high harmonic spectroscopy," Nat. Rev. Phys. **1**(2), 144–155 (2019).
8. R. Cireasa, A. E. Boguslavskiy, and B. Pons, *et al.*, "Probing molecular chirality on a sub-femtosecond timescale," Nat. Phys. **11**(8), 654–658 (2015).
9. D. Baykusheva and H. J. Wörner, "Chiral discrimination through bielliptical high-harmonic spectroscopy," Phys. Rev. X **8**(3), 031060 (2018).
10. D. Baykusheva, D. Zindel, V. Svoboda, E. Bommeli, M. Ochsner, A. Tehlar, and H. J. Wörner, "Real-time probing of chirality during a chemical reaction," Proc. Natl. Acad. Sci. **116**(48), 23923–23929 (2019).
11. S. Ghimire, A. D. DiChiara, E. Sistrunk, U. B. Szafruga, P. Agostini, L. F. DiMauro, and D. A. Reis, "Redshift in the optical absorption of zno single crystals in the presence of an intense midinfrared laser field," Phys. Rev. Lett. **107**(16), 167407 (2011).
12. G. Vampa, T. Hammond, N. Thiré, B. Schmidt, F. Légaré, C. McDonald, T. Brabec, and P. Corkum, "Linking high harmonics from gases and solids," Nature **522**(7557), 462–464 (2015).
13. T. T. Luu, M. Garg, S. Y. Kruchinin, A. Moulet, M. T. Hassan, and E. Goulielmakis, "Extreme ultraviolet high-harmonic spectroscopy of solids," Nature **521**(7553), 498–502 (2015).
14. T. T. Luu and H. J. Wörner, "Measurement of the berry curvature of solids using high-harmonic spectroscopy," Nat. Commun. **9**(1), 916 (2018).
15. S. Ghimire and D. A. Reis, "High-harmonic generation from solids," Nat. Phys. **15**(1), 10–16 (2019).
16. P. M. Kraus, B. Mignolet, D. Baykusheva, A. Rupenyan, L. Horný, E. F. Penka, G. Grassi, O. I. Tolstikhin, J. Schneider, F. Jensen, L. B. Madsen, A. D. Bandrauk, F. Remacle, and H. J. Wörner, "Measurement and laser control of attosecond charge migration in ionized iodoacetylene," Science **350**(6262), 790–795 (2015).
17. H. J. Wörner, C. A. Arrell, and N. Banerji, *et al.*, "Charge migration and charge transfer in molecular systems," Struct. Dyn. **4**(6), 061508 (2017).
18. P. M. Kraus and H. J. Wörner, "Perspectives of attosecond spectroscopy for the understanding of fundamental electron correlations," Angew. Chem., Int. Ed. **57**(19), 5228–5247 (2018).
19. A. L'Huillier, M. Lewenstein, P. Salieres, P. Balcou, M. Y. Ivanov, J. Larsson, and C.-G. Wahlström, "High-order harmonic-generation cutoff," Phys. Rev. A **48**(5), R3433–R3436 (1993).
20. A. Gordon and F. X. Kärtner, "Scaling of kev hhg photon yield with drive wavelength," Opt. Express **13**(8), 2941–2947 (2005).
21. Z. Chang, A. Rundquist, H. Wang, I. Christov, M. Murnane, and H. Kapteyn, "Generation of coherent, femtosecond, x-ray pulses in the "water window"," IEEE J. Sel. Top. Quantum Electron. **4**(2), 266–270 (1998).
22. C.-X. Yun, H. Teng, W. Zhang, M.-J. Zhan, H.-N. Han, X. Zhong, Z.-Y. Wei, B.-B. Wang, and X. Hou, "High-order harmonics generation by few-cycle and multi-cycle femtosecond laser pulses," Chin. Phys. B **19**(12), 124210 (2010).
23. B. E. Schmidt, A. D. Shiner, M. Giguère, P. Lassonde, C. A. Trallero-Herrero, J.-C. Kieffer, P. B. Corkum, D. M. Villeneuve, and F. Légaré, "High harmonic generation with long-wavelength few-cycle laser pulses," J. Phys. B: At., Mol. Opt. Phys. **45**(7), 074008 (2012).
24. T. T. Luu, Z. Yin, A. Jain, T. Gaumnitz, Y. Pertot, J. Ma, and H. J. Wörner, "Extreme–ultraviolet high–harmonic generation in liquids," Nat. Commun. **9**(1), 3723 (2018).
25. Z. Yin, T. T. Luu, and H. J. Wörner, "Few-cycle high-harmonic generation in liquids: in-operando thickness measurement of flat microjets," JPhys Photonics **2**(4), 044007 (2020).
26. V. Svoboda, Z. Yin, T. T. Luu, and H. J. Wörner, "Polarization measurements of deep-to extreme-ultraviolet high harmonics generated in liquid flat sheets," Opt. Express **29**(19), 30799–30808 (2021).
27. A. Shiner, C. Trallero-Herrero, N. Kajumba, B. Schmidt, J. Bertrand, K. T. Kim, H.-C. Bandulet, D. Comtois, J.-C. Kieffer, D. Rayner, P. Corkum, F. Légaré, and D. Villeneuve, "High harmonic cutoff energy scaling and laser intensity measurement with a 1.8 μm laser source," J. Mod. Opt. **60**(17), 1458–1465 (2013).
28. P. B. Corkum, "Plasma perspective on strong field multiphoton ionization," Phys. Rev. Lett. **71**(13), 1994–1997 (1993).

Optics EXPRESS

29. T. Popmintchev, M.-C. Chen, A. Bahabad, M. Gerrity, P. Sidorenko, O. Cohen, I. P. Christov, M. M. Murnane, and H. C. Kapteyn, "Phase matching of high harmonic generation in the soft and hard x-ray regions of the spectrum," Proc. Natl. Acad. Sci. **106**(26), 10516–10521 (2009).
30. M.-C. Chen, P. Arpin, T. Popmintchev, M. Gerrity, B. Zhang, M. Seaberg, D. Popmintchev, M. M. Murnane, and H. C. Kapteyn, "Bright, coherent, ultrafast soft x-ray harmonics spanning the water window from a tabletop light source," Phys. Rev. Lett. **105**(17), 173901 (2010).
31. C. Schmidt, Y. Pertot, T. Balciunas, K. Zinchenko, M. Matthews, H. J. Wörner, and J.-P. Wolf, "High-order harmonic source spanning up to the oxygen k-edge based on filamentation pulse compression," Opt. Express **26**(9), 11834–11842 (2018).
32. M. Lewenstein, P. Balcou, M. Y. Ivanov, A. L'Huillier, and P. B. Corkum, "Theory of high-harmonic generation by low-frequency laser fields," Phys. Rev. A **49**(3), 2117–2132 (1994).
33. A. Mondal, O. Neufeld, Z. Yin, Z. Nourbakhsh, V. Svoboda, A. Rubio, N. Tancogne-Dejean, and H. J. Wörner, "Probing the low-energy electron-scattering dynamics in liquids with high-harmonic spectroscopy," Nature Phys. (in press) (2022).
34. A.-W. Zeng and X.-B. Bian, "Impact of statistical fluctuations on high harmonic generation in liquids," Phys. Rev. Lett. **124**(20), 203901 (2020).
35. C.-L. Xia, Z.-L. Li, J.-Q. Liu, A.-W. Zeng, L.-J. Lü, and X.-B. Bian, "Role of charge-resonance states in liquid high-order harmonic generation," Phys. Rev. A **105**(1), 013115 (2022).
36. J.-X. Chen and X.-B. Bian, "Theoretical analysis of high-order harmonic generation in liquids by a semiclassical method," Phys. Rev. A **107**(4), 043111 (2023).
37. O. Alexander, J. C. T. Barnard, E. W. Larsen, T. Avni, S. Jarosch, C. Ferchaud, A. Gregory, S. Parker, G. Galinis, A. Tofful, D. Garratt, M. R. Matthews, and J. P. Marangos, "The mechanism of high harmonic generation in liquid alcohol," arXiv, arXiv:2202.12624 (2022).
38. O. Neufeld, Z. Nourbakhsh, N. Tancogne-Dejean, and A. Rubio, "Ab initio cluster approach for high harmonic generation in liquids," J. Chem. Theory Comput. **18**(7), 4117–4126 (2022).
39. A. Baltuška, T. Fuji, and T. Kobayashi, "Controlling the carrier-envelope phase of ultrashort light pulses with optical parametric amplifiers," Phys. Rev. Lett. **88**(13), 133901 (2002).
40. J. N. Sweetser, D. N. Fittinghoff, and R. Trebino, "Transient-grating frequency-resolved optical gating," Opt. Lett. **22**(8), 519–521 (1997).
41. M. Lewenstein, P. Salières, and A. L'Huillier, "Phase of the atomic polarization in high-order harmonic generation," Phys. Rev. A **52**(6), 4747–4754 (1955).
42. D. S. Steingrube, T. Vockerodt, E. Schulz, U. Morgner, and M. Kovačev, "Phase matching of high-order harmonics in a semi-infinite gas cell," Phys. Rev. A **80**(4), 043819 (2009).
43. H. Hayashi and N. Hiraoka, "Accurate measurements of dielectric and optical functions of liquid water and liquid benzene in the vuv region (1–100 ev) using small-angle inelastic x-ray scattering," J. Phys. Chem. B **119**(17), 5609–5623 (2015).
44. O. Neufeld and O. Cohen, "Background-free measurement of ring currents by symmetry-breaking high-harmonic spectroscopy," Phys. Rev. Lett. **123**(10), 103202 (2019).
45. A. Schild, M. Peper, C. Perry, D. Rattenbacher, and H. J. Wörner, "Alternative approach for the determination of mean free paths of electron scattering in liquid water based on experimental data," J. Phys. Chem. Lett. **11**(3), 1128–1134 (2020).
46. T. Gadeyne, P. Zhang, A. Schild, and H. J. Wörner, "Low-energy electron distributions from the photoionization of liquid water: a sensitive test of electron mean free paths," Chem. Sci. **13**(6), 1675–1692 (2022).